Magister Thesis

Degree Project in

Marine Geosciences, 45 hp

NEW EVIDENCE FOR A MEGA-EVENT IN THE ARCTIC OCEAN:

ITRAX XRF-SCANNING OF CORES FROM THE YMER-80, ARCTIC OCEAN-96 AND LOMROG-07 EXPEDITIONS

Matteo Mellquist

matteo.mellquist@geo.su.se

Stockholm 2009

Department of Geology and Geochemistry

Stockholm University

106 91 Stockholm

Abstract

During the ice breaker expeditions YMER-80, ARCTIC-96 and LOMROG-07 to the Arctic Ocean several piston and gravity cores were collected. In some of the cores from the Central part of the Lomonosov Ridge a conspicuous, thick, gray homogeneous layer was observed. The color, position and physical properties of this layer make this segment to a significant break in the otherwise yellowish and brown stratigraphy. The formation of this gray feature is here hypothesized to have been caused by an early-middle Weichselian outburst from one of the huge ice-dammed lakes that formed in West Siberia when the Barents-Kara ice-sheet expanded onto mainland Russia.

Using the new X-ray fluorescence (XRF) scanner at Stockholm University, the gray layer could be shown to be characterized by a significant chemical-signature including distinct peaks or minima in Ti, Fe, Ca, as well as a minimum in the redox sensitive element Mn. Out of 38 investigated cores from these tree expeditions, 24 contain a gray unit in the upper 2 m. These 24 cores were taken from the Siberian-, the Central- and the Greenland side of the Lomonosov Ridge as well as from the Gakkel Ridge, the Morris Jesup and the Fram Strait. The presence of the gray layer in these areas thereby gives a prediction of a gray layer in the whole Eurasian Basin. Radiographic images produced on two cores containing the gray layer show a homogeneous, IRD-rich layer with no bioturbation and with a very sharp base boundary. Just below the gray layer in one of the cores an escape trace was observed, indicating a very rapid onset of the deposition of the gray layer.

The extension of this layer together with redox conditions, the escape trace, a sharp base boundary and the grain size of this layer suggest an abrupt deposition resulting in oxygen free condition in the pore waters. Most likely this event was caused by an outburst of an ice-dammed lake.

1. Introduction

During expedition Ymer-80, Arctic Ocean-96 and LOMROG-07 several piston and gravity cores were collected. In some of the cores from the Central part of the Lomonosov Ridge a conspicuous thick, gray homogeneous layer was observed (Jakobsson et al., 2000)(Löwemark et al., 2008), the conspicuous gray layer also observed by (Spielhagen et al., 2004). The color, position and physical properties of this layer, makes this segment to a significant break in the stratigraphy otherwise characterized by yellowish and brown cycles (Jakobsson et al., 2000). The sharp base boundary indicate a fast sedimentation rate and the different appearance compared to the rest of the stratigrapy leads to an idea of some kind of catastrophic-event-origin for this layer. If this is the case, if this layer has been deposited relatively momentary, there must have been a huge force of same kind transporting this enormous amount of material over this area. Potential candidates for this may be a impact of a Meteorite in the Arctic Ocean or the surrounding land, a volcano eruption in the Arctic area, an enormous turbidite, or the origin of this gray layer is the result of an outburst from one of the great ice-dammed lake that formed during the Last Ice Age (Grosswald, 1980). These lakes formed repeatedly between the ice sheet in the north and the continental water divides in south when the ice sheet over the shallow Barents and Kara seas expanded several times on to mainland Russia were the ice front blocked the Siberian north-flowing rivers (Mangerud et al., 2001). An analogue to this event is the freshwater outburst of Lake Agassiz (Kennett and Shackleton, 1975) when the formation of North Atlantic Deep Water was strongly reduced for 100 years and corresponds to the most extreme climate anomaly during Holocene dated at 8200 B.P. (Kleiven and O. Richter, 2008).
The great outburst of the ice dammed lakes in Siberia and the gray layer found in the arctic sediments could provide a much needed connection between land and ocean as suggested by (Mangerud et al., 2004).
The aim of this study is to pin-point the geographic and stratigraphic extensions, as well as the genesis, of this gray layer using the new X-ray-fluorescence (XRF) core scanner at Stockholm University to examine 38 sediment cores, 7 cores from expedition YMER-80, 21 cores from ARCTC OCEAN-96 and 10 cores raised during expedition LOMROG-07.

2. Background

2.1 Physiography

The Arctic Ocean is a relatively small ocean, making up only 1 % of the world ocean's volume. The Arctic is characterized by its large shelves; 52.7 % of the area is made up by shallow shelf areas, 30 – 50 m deep, while the abyssal plains constitute no more than 14.1 %, ridges 15,8 %, rises 11.5 % and continental slopes 5,7 %, the residual 0.2 % consist of so-called isolated basins (Jakobsson et al., 2003).
The shelves of the Arctic Ocean can be subdivided into seven seas: the Barents-, Kara-, Laptev- and East Siberian Sea on the huge shelf direct north of Siberia, the Chuchi Sea on the shelf north of Bering Strait, the Beaufort Sea located between Alaska and the North Canadian Archipelago, and finally the Lincoln Sea between Greenland and the Lomonosov Ridge. The great Lomonosov ridge divides the Arctic Ocean in to two main basins; the Eurasian Basin and the Amerasian Basin. The Eurasian Basin is then subdivided by the Gakkel Ridge in to Amundsen Basin and Nansen Basin. The Amerasian Basin can be subdivided by Alpha Ridge and Mendeleev Ridge into the Canadian Basin and the Makarov Basin.

2.1.1 Lomonosov Ridge

The Lomonosov Ridge is a deep-sea ridge that stretches from north of Greenland across the entire Arctic Ocean to the Siberian Continental margin near the New Siberian Islands. This ridge is well over 1500 km long, 50–70 km wide, and rises from the surrounding 4000-4200 m deep abyssal plains up to almost 600 m below sea level at its shallowest parts. The ridge is a continental margin that was separated by rifting from the Barents-Kara Sea shelf starting around the Paleocene/Eocene boundary (~56 Ma) when the Eurasian Basin began to form (Vogt et al., 1979).

2.1.2 Yermak Plateau and Morris Jesup Rise

The Yermak Plateau is a shallow marginal plateau north-west of Spitsbergen. This plateau is a composite of both oceanic and continental crust; the southern part is of continental origin formed in a triple junction north of Greenland (Jackson, 1984). The northern part is of oceanic origin and formed in conjunction with the Morris Jesup Rise when the North America, Greenland and the Eurasian plate were initially moving and split the Icelandic-like precursor of these plateaus in two parts. The southeastern part followed the Eurasian side of the Gakkel Ridge to become the Yermak Plateau, while the northwestern part became the Morris Jesup Rise (Jackson, 1984).

2.1.3 Gakkel Ridge

The 1800 km long ultraslow spreading ridge which bisects the Eurasian basin is an extension of the Mid-Atlantic Ridge, to which it is linked by an unnamed short ridge in the Greenland Sea (Sohn et al., 2008). The Gakkel Ridge is taking up 3,1 % of the Arctic Ocean with a calculated are of 295000 km^2 (Jakobsson, 2002).

2.1.4 Fram Strait

The Fram Strait between Greenland and Spitsbergen is the only deep sea connection between the North Atlantic and the Arctic Ocean. This narrow strait, 2000-3000 m deep, is the main exchange gate for water masses, sea ice and heat flux between the Arctic Basin and the sub-Arctic seas (H. Sagen, 2008).

2.2 Oceanography

The surface currents' affecting the ice movement in the Arctic Ocean is mainly consisting of the Trans Polar Drift (TPD) on the Eurasian side of the Ocean, and the Beaufort gyre on the Amerasian side (fig 1). The Trans Polar Drift begins on the Siberian shelf, crosses the whole Arctic Ocean and continues down through the Fram Strait and out in to the Greenland Sea. The path of the TPD across the Arctic is changing in an oscillating manner (fig. 1) depending on the North Atlantic Oscillation (NAO) and the Arctic Oscillation (AO). The NAO is a north-south fluctuation in air masses over the North Atlantic, often given as the NAO-index, while the Arctic Oscillation is a fluctuation of air masses between mid and high latitudes around the whole Northern Hemisphere. The NAO and AO taken together give the vorticity index. If the vorticity is in a positive mode, the Transpolar Drift bends over into the Amerasin Basin (red arrow in fig 1). In contrast, a negative mode results in the TPD trajectory being shifted towards the Eurasian Basin (blue arrow in fig. 1). This regime shift has been happening in a 40-60 year

oscillation during the last century (Mysak, 2001). The Beaufort gyre is a clock-wise rotating current in the Amerasian side of the Arctic Ocean (fig. 1). (Aagaard, 1995). These surface currents affect the Arctic Surface Water (ASW) that mainly consist of North Atlantic water, Pacific water and runoff from the big Siberian rivers Lena, Ob, Yenisey, Pechora, Severnaya and Kolyma. This Surface water that makes up the first 50 m of the water column in the Arctic Ocean is relatively low in salinity and quite cold (Peterson et al., 2002).

.

2.3 Sedimentation

The central Arctic Ocean sediments consist of particles ranging in size from clay to large drop stones. Clay particles can be transported long distances by wind or stay in suspension for years and be transported across the ocean by currents. In order to transport particles substantially larger than the clay size fraction from the shelf areas out to the deep central Arctic Ocean, sea ice or glacier ice is needed as a transport mechanism (Clark, 1970). Once the sediment particles are incorporated in the sea ice or glacial icebergs, the ocean currents govern the transport pathway from the sediment source area. In turn, the surface current and ice drift is heavily affected by the wind pattern.

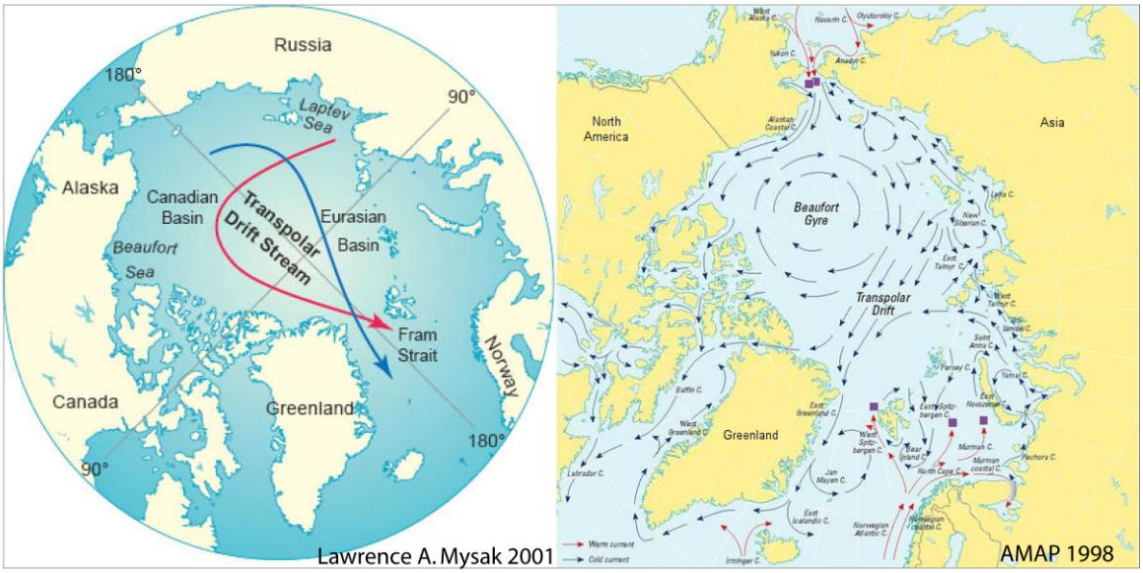

Fig. 1. Left image: the two paths for the Transpolar Drift. Clockwise (blue curve) associated with negative vorticity index and counter clockwise (red curve) positive vorticity index. Right image: the main surface currents, Transpolar Drift in the Eurasian Basin and the Beaufort Gyre in the Amurasian Basin. Blue curves = cool streams and red curves = warm Atlantic water streams. (AMAP 1998)

The shallow shelf areas surrounding the Arctic Ocean represent a highly dynamic environment through the Pleistocene, due to large variations in sea level, river discharge (Stein, 1998) and the formation and decay of major ice sheets (Eiliv Larsen, 1999). The clastic sedimentation at the ridges in the central Arctic Ocean is a direct result from sea- and glacier ice activity, driven by surface currents, meaning that the sediments in the Arctic constitute archives containing information on the Arctic Ocean glacial-interglacial fluctuations and paleoceanography (Spielhagen et al., 1997).

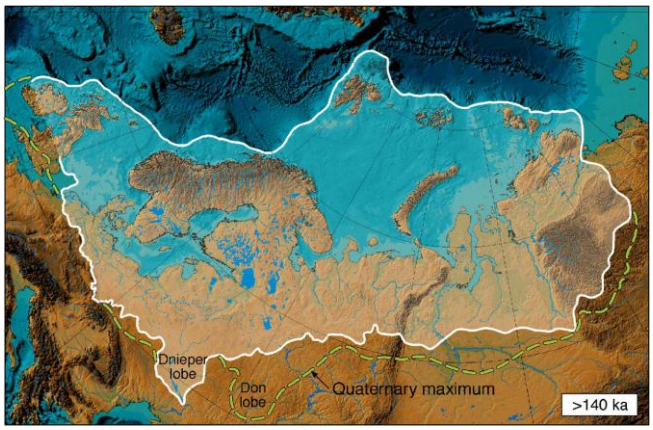

Fig. 2. The dashed line shows the ice-sheet maximum during the Late Saalian 160-140 ka, a reconstruction. Dotted line shows an approximation of the overall Quaternary ice maximum(Svendsen et al. 2004).

2.4 Ice sheet history of the Eurasian side of Arctic

During the last 160 ka at least four major glaciations have affected Northern Eurasia, one time in the Late Saalian and tree times in the Weichselian (Svendsen et al., 2004). The Saalian and the Late Weichselian (LGM) ice extensions are fairly well known on the European mainland but still major uncertainties exist for the other ice-sheets with extensions smaller than the Saalian and LGM.

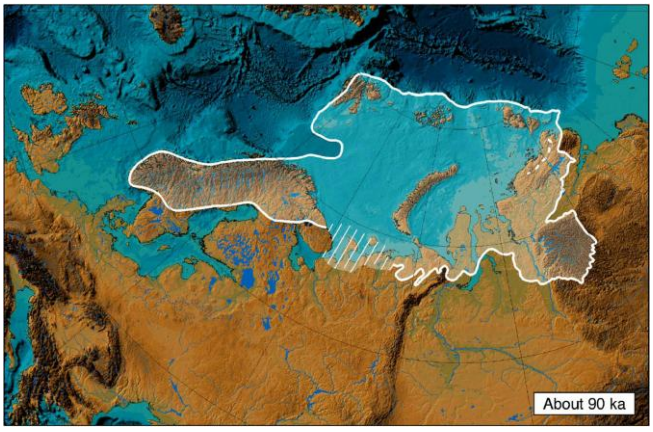

Fig. 3. The dashed line shows the ice-sheet extension during the Early Weichselian glacial maximum (90-80 ka.). Hatched field between Pechora Lowland and the Kola Peninsula: position of ice-margin unknown (Svendsen et al. 2004).

Late Saalian 160–130 ka, MIS 6 (fig. 2). The most extensive and longest lasting Quaternary ice-sheet formed over Northern Eurasia. A huge ice-sheet that stretched from the shelf break in the Norwegian Sea (Mangerud et al., 1998) down to the British Islands in the west, and far south-east in Russia (Svendsen et al., 2004). The enormous ice shelves in front of this ice sheet probably caused large scale erosion on the Central Lomonosov Ridge in north (Jakobsson, 1999).

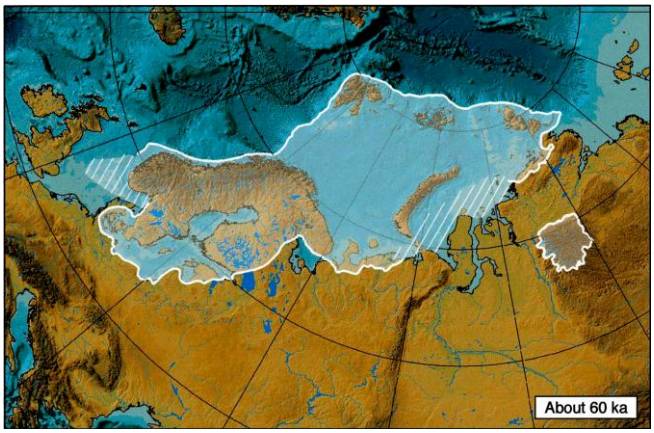

Fig. 4. The dashed line shows the ice-sheet extension during the Middle Weichselian glacial maximum (60-50 ka.). Hatched field: position of ice-margin unknown (Svendsen et al. 2004).

Early Weichselian 100-80 ka, MIS 5d-5b (fig. 3). A large ice-sheet extending

from the south of Norway, following the east coast of the ice-free Baltic Sea in west to the Putorana Plateau in east, covering the shelf of the Barents and Kara seas. During the glacial maxima this ice is thought to have been over thousand meter thick at the North-West coast of the Taimyr Peninsula causing a sea level lowering of 50 m (Lambeck et al., 2002) (Fig. X). (Svendsen et al., 2004).

Middle Weichselian 60-50 ka, MIS 4-3 (fig. 4). After the interstadial sub stage MIS 5a, a regrowth of the ice-sheet during MIS 4 led to a new ice-advance in to mainland Russia, with less extension in the eastern part of Siberia, with no connection to the ice on the Putorana Plateau, but with a larger extension in the west covering the entire Scandinavia, Finland the Baltic Basin as well as part of the white Sea Basin. This glaciations was followed by a major deglaciation with ice-free shelves during 50-30 ka in the Barents Kara-region (Fig. X). (Svendsen et al., 2004).

Late Weichselian 25-10 ka, MIS 2 (fig. 5). During the Late Weichselian glacial maximum 20-15 ka (LGM) the ice-sheet were spread further west compared to the Early and Middle Weichselian ice-sheets, with an ice-margin eastward in the middle of the Kara Sea, and the British Islands to the west. This ice was covering the main part of the Nordic Sea, the entire Baltic and the Barents Sea (Svendsen et al., 2004).

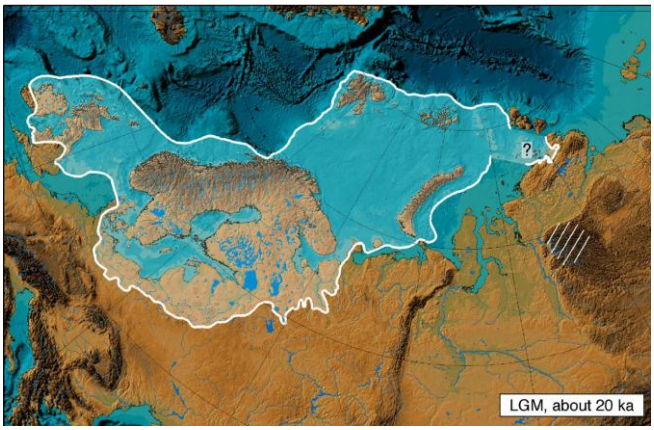

Fig. 5. A reconstruction of the ice-sheet extension during the Late Weichselian glacial maximum (LGM) (Svendsen et al. 2004).

2.5 Ice-age lakes in Northern Siberia

The great Siberian rivers Ob, Yenissei, Pecora and Mezen were blocked several times when the extensive ice sheet over Barents and Kara Sea expanded onto the Siberian mainland. Between the ice edge and the water divide farther south, several big ice dammed lakes were formed. By mapping and OSL dating the ancient shorelines, the extension of these lakes were reconstructed (Mangerud et al., 2004). These lakes are thought to have collapsed and drained in a similar way as the modern outburst from the Grímmsvötn reservoir in Iceland were the pressure of the water lifted the ice and created subglacial tunnels (Björnsson, 2002).

1) On the Pecora Lowland a big ice dammed lake named Lake Komi with a surface 90 – 110 m a.s.l., an area of 76×10^3 km^2 and a volume of 2.4×10^3 km3 is thought to have existed during MIS 5b, about 90-80 ka ago. An outburst of Lake Komi is suggested to have occurred over a few months with a flood path following the present valley of the Pecora River out in to the Barents Sea (Mangerud et al., 2004).

2) The Lake on the West Siberian Plain is not very well mapped or dated. Mangerud et al (2003) have modeled two stages of this lake: A) the first model of this lake in MIS 5d – 5a, 90 - 80 ka with a postulated level of 60 m a.s.l., an area of 610×10^3 km^2, and with a volume of 15 ×

10^3 km^3. B) Second stage in MIS 4-3, 60 -50 ka an estimated lake with surface level of 45 m a.s.l., an area of 45×10^3 km^2 and a calculated volume of 32×10^3 km^3.

3) The Lake in the White Sea Basin was formed between the Timan Ridge and the ice sheet in the White Sea Basin about 90-80 ka with a surface level of 100 m.a.s.l, an area of 218 $*10^3$ km^2 and a volume of 15×10^3 km^3. A plausible drainage way is south to Volga and further out in the Baltic (Mangerud et al., 2004).

3. Material and Methods

3.1 Cores

In this study a total of 38 piston- and gravity cores were analyzed for elemental variations using the ITRAX X-ray fluorescence scanner at Stockholm University (fig. 8).

In the area around Spitsbergen, Fram Strait and Yermak Plateau 41 sediment cores were successfully raised during expedition YMER-80 (Boström and Thiede, 1984). Out of these 41 cores, 7 cores in a transect from northwest to southeast were selected for this study (fig. 7).

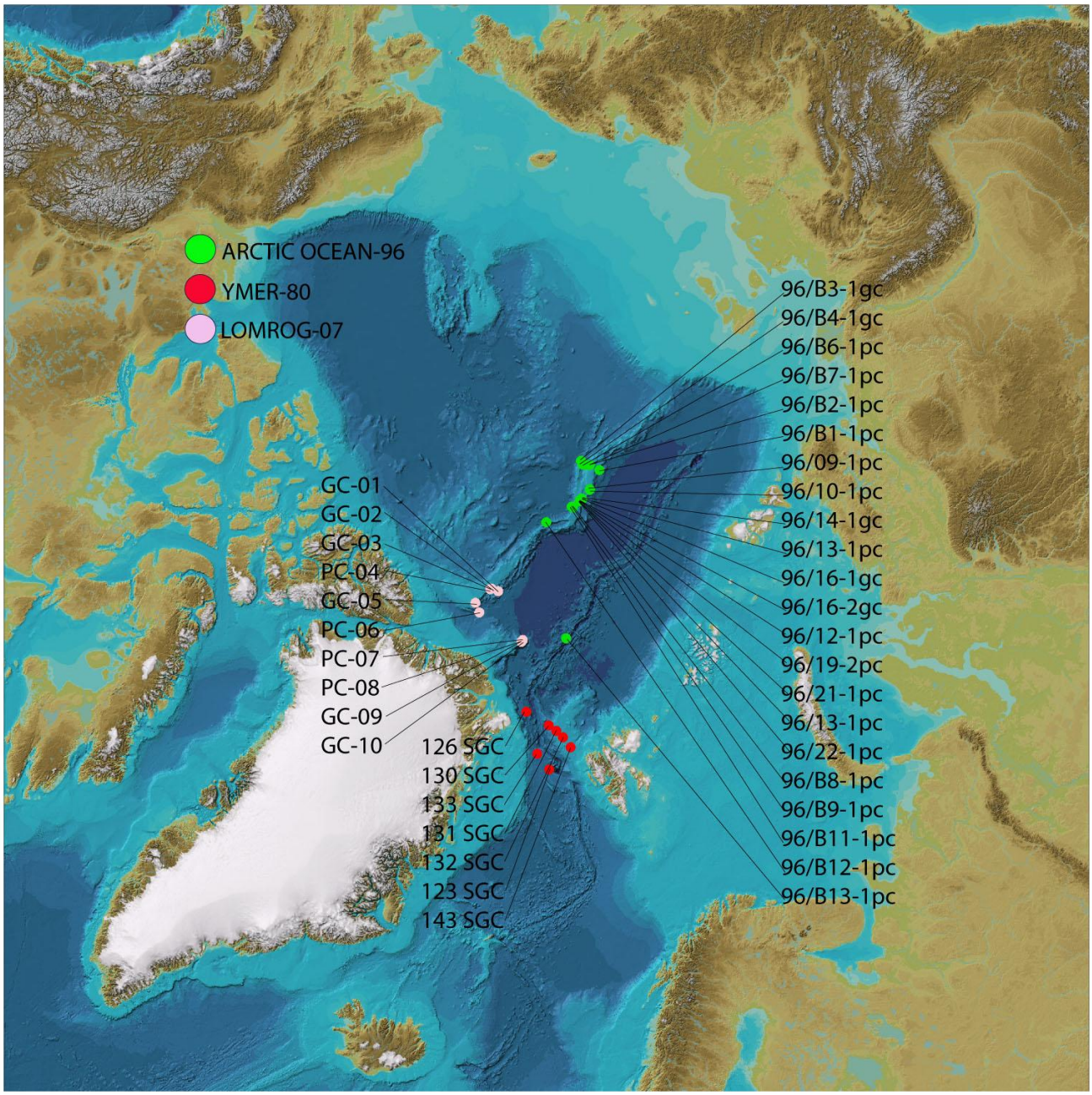

Fig. 7 Coring sites with core-ID. Green dots for cores raised during expedition ARCTIC OCEAN-96, red dots for YMER-80 and pink dots for LOMROG-07.

During expedition Arctic Ocean-96, 21 cores from the Central Lomonosov Ridge were raised using Stockholm University piston/gravity corer (Jakobsson et al., 2001). All these 21 cores were used in this study (fig. 7). The same coring equipment used during Arctic Ocean- 96 was used to raise 10 piston and gravity cores during expedition LOMROG-07 (Jakobsson, 2008) (fig. 7). The first 6 cores were taken on the Greenland side of the Lomonosov Ridge and 4 cores on the Morris Jesup Rise. These 10 cores were all analyzed with the ITRAX in this study.

3.2 X-ray fluorescence

X-ray fluorescence (XRF) is a non-destructive, fast analytical method to determine the chemical composition of all kind of materials. The XRF works according to the following basic principle: a sample is hit by X-ray radiation, this causes the elements in the sample to emit fluorescent X-ray radiation with discrete energies characteristic for the different elements in the sample. By measuring the energies and the intensity of the radiation from the sample it is possible to determine which elements are present and the relative amount of each element (Brouwer, 2003).

The characteristic fluorescence is produced when, using a classical atom model, an X-ray photon from the source with sufficient energy are hitting and expelling an electron in e.g. the K-shell, making the atom in the sample instable with a higher energy. The atom restores the hole in the K-shell by taking an electron from e.g. the L-shell back to the K-shell. When an electron from the L-shell is transferred to the K-shell it is moved from a higher energy state to a lower. This surplus energy is adjusted by sending off a photon, the X-ray luminescence (Brouwer, 2003).

3.3 ITRAX

The ITRAX-Core Scanner is a new automated multi-function core scanning instrument designed to gather micro-X-ray fluorescence spectrometry (µXRF) elemental profiles, optical and micro radiographic images in the same run from the same sediment section. It can operate on split cores of both soft sediments and rock samples from a few centimeters to a maximum length of 180 cm, and acquire data at a resolution as fine as 200 µm. The split core is advanced by a programmable stepped motor drive trough the measurement tower on a transport bed (fig. 8). The measurement tower consist of a X-ray focusing unit, an optical line camera, a laser topographic scanner, an X-ray line camera and a high count-rate XRF detection system.

Fig 8. The ITRAX multi-function core scanner.

The scanning procedure is controlled from the Core Scanner Navigator program in an external computer.

The XRF spectra produced are automatically analyzed by the Q-spec program, and the individual peak areas for the specific elements are calculated to allow an on-the-fly evaluation of the measured data Q-spec is also used to refine the analysis after the scanning procedure is completed (Ian W. Croudace, 2006).

3.4 X-Ray

Samples for radiographies were taken from core 96/14-1pc and LOMROG07-GC-10. Small plastic boxes were pressed down into the split core and cut out by pulling a nylon string underneath the boxes, which could then be carefully removed, this method is described in (Löwemark and Werner, 2001). The sediment filled plastic boxes were placed directly on X-ray film and exposed to 55 kV for 3 min at the X-ray facility at the University of Bremen.

3.5 Physical properties

All 10 cores raised on expedition LOMROG-07 were directly measured on board the icebreaker Oden using the Geotek Multi Sensor Core Logger (MSCL) from the Core processing lab at Stockholm University (Jakobsson, 2008). The MSCL measures Magnetic susceptibility, P-wave velocity, and GRAPE density. This technique was unfortunately not yet invented when the cores from YMER-80 expedition were raised. On the cores from the Arctic Ocean 96 cruise, MSCL measurements were made on cores 96/09-1pc, 96/10-1pc, 96/12-1pc, 96/13-1pc, 96/B8-1pc and 96/B2-1pc (Jakobsson et al., 2001) Using the machine at the Bedford Institute of Oceanography in Halifax.

4. Results

4.1. Anatomy of the Gray Layer

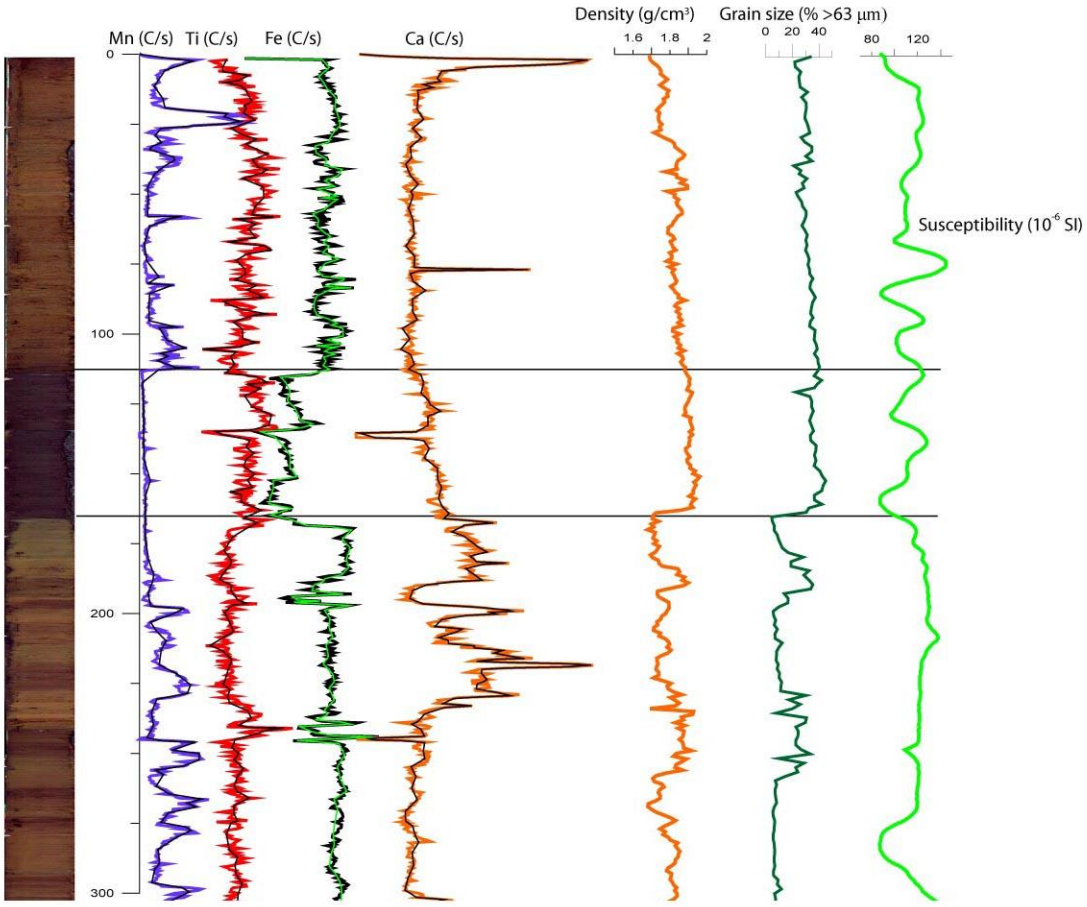

Fig. 9 From left to right: The reference core 96/12-1pc, with the gray layer in the middle marked by the black horizontal lines. Mn (blue), Ti (red), Fe (green) and Ca (orange) together is making up the chemical fingerprint used to identify the gray layer. The lines inside the colored are spline smoothing functions to make the fluctuations clearer. To the right, density (orange), grain size > 63µm (dark green) and susceptibility (light green).

Core 96/12-1pc (fig. 9) has previously been selected as a key core for the Lomonosov upper sediment stratigraphy and age model construction due to undisturbed acoustic stratigraphy with no obvious indication of erosion (Jakobsson et. al 2001). 96/12-1pc is one of the cores were the gray layer first was observed, and in this study it is used as a reference core. This core shows a ca 45 cm distinct dark homogeneous gray layer, an abrupt change in the otherwise yellow-brown stratigraphy. The XRF-data for this section shows a significant decrease in Fe and an increase in Ti trough the whole gray section, Mn is the element showing the most outstanding change, with counts close to zero through this section and 15 cm further down.

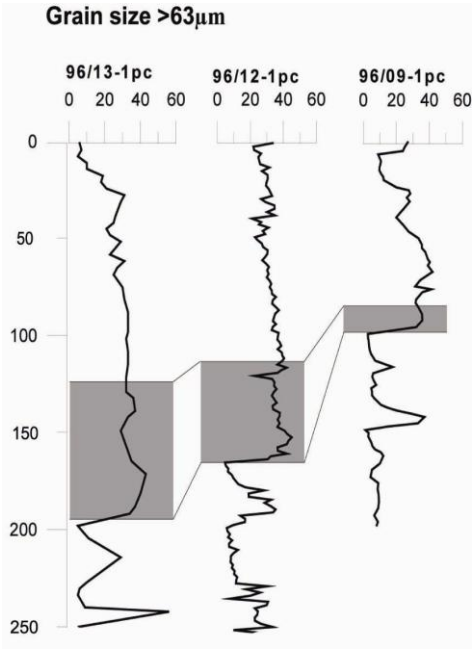

Fig. 10. Grain size >63 µm (%). The significant increase in grain size corresponds well to the base boundary of the Gray Layer. The increase forms an obvious boarder between the two different grain size regimes. The Gray Layer marked with gray boxes.

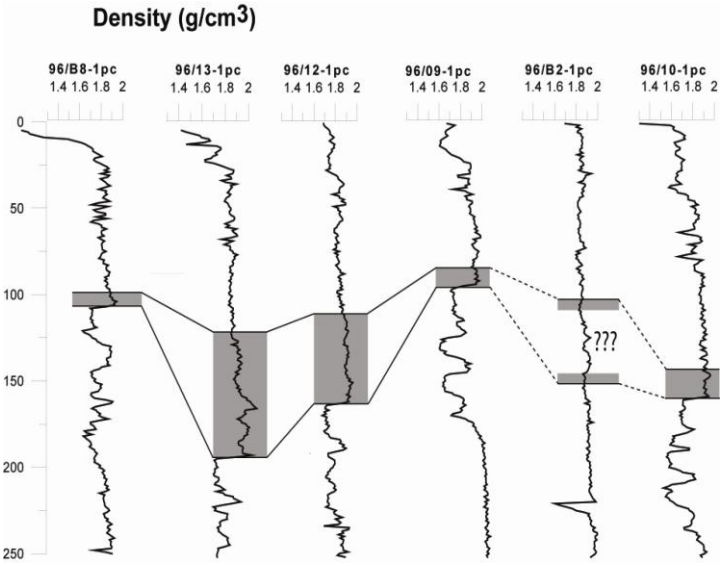

Fig. 11. Gamma density (g/cm^3). The gray transparent boxes show the position of the Gray Layer. The sharp base boundary of the layer corresponds well with the significant increase in density except for core 96/B2-1pc.

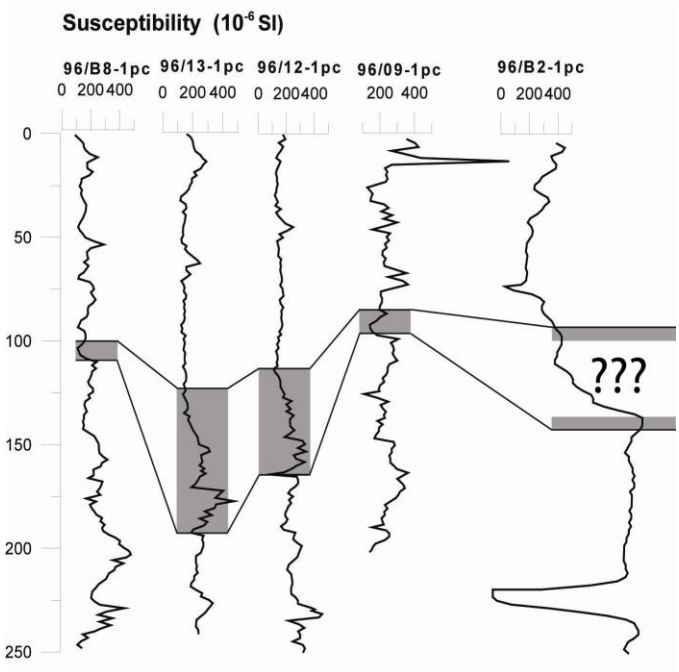

Fig. 12. Magnetic Susceptibility (10^{-6} SI). The base boundary of the Gray Layer corresponds with a small dip in susceptibility but else doesn't show any significant signature. 96/B2-1pc differs from the other cores and doesn't contain any identifiable Gray Layer. The Gray Layer marked with gray boxes.

The stratigraphic position of the sharp base boundary is also marked by a closure of a ca 75 cm Ca peak interval beneath the gray layer.

Grain size analyses were done on core 96/13-1pc, 96/12-1pc and 96/09-1pc (fig. 10) by wet sieving (Jakobsson et. al 2001). The fraction >63µm shows an abrupt change at the base boundary in all of the three cores with significantly higher contents above and further to the top of the cores (fig. 10). The Gamma density (fig. 11) and P-wave velocity shows a pattern like the grain size profile; an abrupt increase at the base boundary that continue upwards. The Magnetic Susceptibility on the other hand exhibits a sharp dip just at the boundary (fig. 12).

XRF-data together with digital core pictures and the physical properties are used as a fingerprint to identify this gray layer in the other cores. Exceptions in the gray layer's chemical characteristics, position, length and optical appearance

compared with 96/12-1pc are briefly described below.

4.1.1 Central Lomonosov Ridge

Cores on the Central Lomonosov Ridge (table 1) can be subdivided in three groups:

1) Table 1. Cores taken on the Oden Spur and on the Lomonosov Ridge directly west of the Oden Spur, cores 96/B1-1pc – 96/B7-1pc around 85º North. The Gray Layer is only present in core 96/B1-1pc, taken from the Eurasian edge of the Ridge. Core 96/B1-1pc shows a Mn decrease and a Fe decrease corresponding to a ca 10 cm visible dark gray part with a sharp base boundary, although not as sharp as in the reference core. Core 96/B1-1pc has no trace of the Ca peak area present beneath the gray unit as in the reference core. No MSCL data available.

2) Table 1. Cores taken farther north, around 87ºN, 96/09-1pc – 96/22-1pc, on the Eurasian side of the crest of the ridge, including the reference core 96/12-1pc, clearly show a dark gray layer with the characteristic chemical and physical fingerprint. This gray part range in length from a few cm in core 96/16-2gc up to 70 cm in core 96/21-1pc, even the position of the sharp base boundary in the cores varies quit a lot from a core depth of 28 cm in core 96/19-2pc down to 200 cm in core 96/21-1pc.
The Ca peak area that ends at the base boundary of the Gray Layer in 96/12-1pc is not seen or is not that distinct in cores 96-09, 10, 13 and 16-1.
Cores 96/B8-1pc, 96/B9-1pc and 96/B11-1pc were taken on the Canadian side of the Lomonosov Ridge. All three display a gray unit, much lighter and with a base boundary not as sharp as the reference core, just above 100 cm. The Mn part of the chemical signature shows a minimum, but not that distinct as the reference core. Ti, Fe and Ca all show the same pattern as the reference core. Physical properties of core 96/B8-1pc (Backman et al., 2004) show the typical increase in density and a peak in magnetic susceptibility corresponding to the gray layer.

3) Table 1. Core 96/B12-1pc taken on the Canadian edge of the intra basin shows a diffuse gray layer around 100 cm with a dip in Fe, a minimum in Mn but without any significant increase in Ti.. The layer is much shorter compared to the reference core, The Layer's base boundary is not very sharp but corresponds well with the top of the Ca peak area.

Table 1. 21 cores from theARCTIC OCEAN-96 expedition XRF-analyzed in this study. In the header from left to right: Core-id number and type of gear, pc – Piston Core and gc – Gravity Core. Area – coring site with coordinates. Water depth beneath sea surface (m). Sediment recovery - net length of the raised core (m). The Gray Layer identified by the chemical fingerprint, physical properties, grain size and optical distinction, occurrence - Yes or No.

Core ID	Area	Latitude	Longitude	Water depth (m)	Sediment recovery (m)	The Gray Layer
96/09-1pc	Lomonosov Ridge	143,44	86,41	-927	2,93	Yes
96/10-1pc	Lomonosov Ridge	143,18	86,44	-947	3,42	Yes
96/12-1pc	Lomonosov Ridge	144,77	87,10	-1003	7,81	Yes
96/13-1pc	Lomonosov Ridge	145,17	87,15	-978	4,73	Yes
96/14-1gc	Lomonosov Ridge	143,67	87,01	-1941	3,87	Yes
96/16-1gc	Lomonosov Ridge	144,48	87,01	-1445	3,86	Yes
96/16-2gc	Lomonosov Ridge	144,43	87,02	-1405	2,48	Yes
96/19-2pc	Lomonosov Ridge	144,64	87,12	-991	9,00	Yes
96/21-1pc	Lomonosov Ridge	144,67	87,14	-987	5,81	Yes
96/22-1pc	Lomonosov Ridge	144,68	87,14	-980	6,00	Yes
96/B1-1pc	Lomonosov Ridge	145,76	85,39	-2525	9,55	Yes
96/B2-1pc	Lomonosov Ridge	152,28	85,41	-611	3,87	No
96/B3-1gc	Lomonosov Ridge	158,31	85,42	-2353	2,20	No
96/B4-1gc	Lomonosov Ridge	158,06	85,40	-1875	5,20	No
96/B6-1pc	Lomonosov Ridge	154,64	85,50	-2094	4,11	No
96/B7-1pc	Makarov Basin	156,60	85,55	-2385	7,80	No
96/B8-1pc	Lomonosov Ridge	146,88	87,62	-1261	6,38	Yes
96/B9-1pc	Lomonosov Ridge	148,36	87,62	-1785	6,50	Yes
96/B11-1pc	Lomonosov Ridge	148,43	87,62	-1819	6,50	Yes
96/B12-1pc	Lomonosov Ridge	179,60	88,72	-1854	6,39	Yes
96/B13-1pc	Gakkel Ridge	12,54	85,52	-2079	1,65	Yes

4.1.2 Gakkel Ridge

Table 2. 96/B13-1pc shows two gray parts in the upper 100 cm of the core. The upper 20 cm long gray interval has a distinct base boundary at 50 cm. The lower gray unit is around 10 cm long, with its base, not as sharp as in the reference core, at 70 cm. There is a Mn minimum that stretches from the top of the upper layer down trough both gray layers, but with a peak at the top of the lower layer. The upper gray part doesn't show the typical pattern in Ti, Fe or Ca. The lower, on other hand, shows the characteristics of the Gray layer, but less distinct compared with 96/12-1pc.

4.1.3 Yermak Plateau and Fram Strait

Table 2. Out of the 7 cores analyzed from the Yermak Plateau and Fram Strait, 123 SGC is the only core from this area showing something like the Gray Layer with a clear minimum in Mn and a base boundary that corresponds with the end of the Ca peak area like 96/12-1pc. Ti display a slight increase trough the layer, Fe however, has a small dip just at the boundary.

Table 2. 7 cores from expedition YMER-80 chosen for XRF-analysis in this study. In the header from left to right: Core-id number and type of gear, SGC – Super Gravity Core. Area – coring site with the coordinates. Water depth beneath sea surface (m). Sediment recovery - net length of the raised core (m). The Gray Layer identified by the chemical fingerprint and optical distinction, occurrence - Yes or No.

Core ID	Area	Latitude	Longitude	Water depth (m)	Sediment recovery (cm)	The Gray Layer
123 SGC	Fram Strait	79,23	0,80	-3050	8,80	Yes
126 SGC	Fram Strait	82,00	-6,92	-3362	2,15	No
130 SGC	Yermak Plateau	81,40	0,87	-1590	4,13	No
131 SGC	Yermak Plateau	81,12	3,20	-820	3,49	No
132 SGC	Yermak Plateau	80,78	5,12	-680	4,70	No
133 SGC	Fram Strait	80,02	-2,47	-2690	2,99	No
143 SGC	Yermak Plateau	80,27	7,03	-560	3,45	No

4.1.4 Greenland side of Lomonosov Ridge

Table 3. Out of six cores from this area, three cores, GC-02, GC-03 and PC-04 display an identifiably Gray Layer. In core GC-02 this layer is round 10 cm thick and has its sharp base boundary at 35 cm depth, at the top of the Ca peak. Mn shows a shorter and less distinct minimum compared with core 96/12-1pc, Fe and Ti also differ and don't show the chemical characteristics as the reference core. The gray layer in PC-04 is also around 10 cm but have its base boundary at a depth of 94 cm with an even less distinct minimum in Mn, but with a typical signature in Fe and Ti. Core GC-03 displays a gray unit that begins at ca 12 cm and continues up to the top of the core with a similar chemical signature as in the other two.

4.1.5 Morris Jesup Rise

Table 3. GC-10 and GC-09 were taken close to each other, both show an apparent gray layer with the base boundary just above 50 cm, the layer is about 15 cm in core GC-10 and just a few cm in GC-09. The Ca peak that ends at the base boundary of the layer is even more distinct in these two cores compared to 96/12-1pc. Fe shows a decrease as in 96/12-1pc but no significant increase in Ti. Core PC-07 and PC-08 show a traceable Gray Layer 5-7 cm thick at 90 respective 50 cm depth. Both correspond well with the Ca and Fe profiles but the Mn shows a peak in the layer and a minimum beneath. Ti shows no significant increase within the layer. A sharp density increase corresponds well with the reference core in all four cores.

Table 3. 10 cores from expedition LOMROG-07 XRF-analyzed in this study. In the header from left to right: Core-id number and type of gear, PC – Piston Core and GC – Gravity Core. Area – coring site with coordinates. Water depth beneath sea surface (m). Sediment recovery - net length of the raised core (m). The Gray Layer identified by the chemical fingerprint, physical properties, and optical distinction, occurrence - Yes or No.

Core ID	Area	Latitude	Longitude	Water depth (m)	Sediment recovery (m)	The Gray Layer
GC-01	Lomonosov Ridge	86,15	-48,15	-1573	1,47	No
GC-02	Lomonosov Ridge	86,63	-54,15	-723	2,43	Yes
GC-03	Lomonosov Ridge	86,63	-54,96	-721	1,98	Yes
PC-04	Lomonosov Ridge	86,70	-53,77	-811	5,49	Yes
GC-05	Lomonosov Ridge	85,65	-52,45	-1440	2,85	No
PC-06	Lomonosov Ridge	85,49	46,27	-3009	4,18	No
PC-07	Morris Jesup rise	85,40	-14,28	-1252	4,68	Yes
PC-08	Morris Jesup rise	85,32	-14,86	-1038	6,03	Yes
GC-09	Morris Jesup rise	85,29	-14,89	-1016	2,34	Yes
GC-10	Morris Jesup rise	85,29	-14,81	-1017	2,58	Yes

4.2 X-ray radiography

Core 96/14-1pc.

The sharp base boundary at 167 cm in core 96/14-1pc appears very distinct in the radiography. The sediments instantly change from dark homogeneous well bioturbated sediment just beneath the boundary to a light homogeneous material. The boundary is enhanced by ice rafted debris like a chaplet just on top of the sharp edge. The material in the gray layer displays bigger grains, a lot of ice rafted debris and no bioturbation in the first 12 cm. Additionally, just below the boundary a 4 cm tubular trace appears. Bromley (1996) describe similar features like this to be escape structures, produced when endobenthic organisms try to escape burial caused by rapid sedimentation events.

Core GC-10.

The edge of one sample box used for the radiographies was just hitting the Gray Layer base boundary in core GC-10. The material beneath the boundary is a mixture of coarser grains and fine material with a mottled, strongly bioturbated sediment. Above the boundary the sediment is very homogeneous, the sediments consists of a sandy material with a lot of ice rafted debris and no sign of bioturbation. In the very top of the second box, ca 15 cm above the boundary, a light horizontal lineation appears and continues upwards.

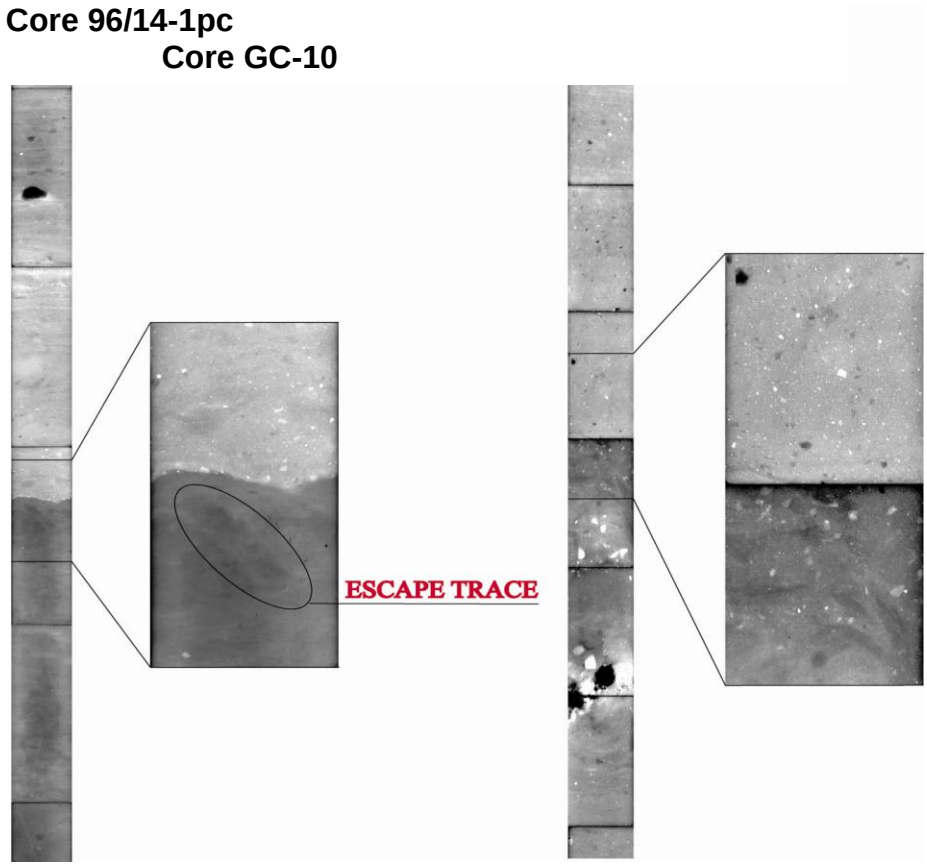

Fig. 14. X-ray images of the Gray Layer in core 96/14-1pc and GC-10 shows a sharp base boundary with a homogenous non bioturbated material above and a mottled material beneath with intense bioturbation. 96/14-pc shows an escape trace just beneath the boundary.

5. Discussion

5.1 The geographical extension of the Gray Layer

Out of the 38 investigated cores from the three expeditions, 24 contain the gray unit in the Out of the 38 investigated cores from the three expeditions, 24 contain the gray unit in the upper 2 m. These 24 cores are representative for the stratigraphy of the Eurasian side of the Lomonosov Ridge as well as the Gakkel Ridge, the Morris Jesup Rise and the Fram Strait. In the present Arctic Ocean circulation setting, the area where the gray layer occurs is primarily influenced by the Transpolar Drift. Previously established age models for the central Arctic Ocean cores suggest that the gray layer was deposited during Marine Isotope Stage 4 (MIS 4) (Jakobsson et al., 2001), however, this age assignment must be considered uncertain as no chronological tie points exist directly in, above or below the gray layer. Spielhagen et al. (2004) describe "*A thick IRD-rich layer deposited in the younger part of OIS 4 and oldest OIS 3 is one of the most conspicuous feature in sediments cores from the eastern and central Arctic Ocean*" the sharp base boundary and the sharp increase in fraction >63 μm in this conspicuous layer are features among others used to correlate seven cores, PS1535, PS1533-3, PS2200, PS2185, PS2178 and PS51/038-4, taken in a transect from the Fram Strait to the Mendeleev Ridge including the reference core 96/12-1pc. This conspicuous layer, which correlates well with the Gray Layer, is said to be identified in all of these seven cores (Spielhagen et al., 2004). Thereby not sure, but likely, that the increase in grain size indicate the same gray layer in the core from the Amerasian side of the Arctic as the cores from the Eurasian. Cores taken on the Greenland side and Amerasian margin of the Lomonosov Ridge and the Oden Spur tend to hold a weaker gray layer, less distinct in color but with the same chemical fingerprint, suggesting an extension for the gray layer in the Eurasian Basin into the most distal part at the Makarov Basin margin of the Lomonosov Ridge.

5.2 The stratigrapic position of the Gray Layer

The Gray Layer range in thickness from a few cm up to 70 cm in core 96/21-1pc. Core 96/19-2pc shows a ca 30 cm gray layer in the very top of the core, this is probably due to imploded liner and disturbed upper part of the core (p.com Jakobsson M. 2008). These variations are in short distances, but the overall pattern shows the thickest layer on the Central Lomonosov Ridge and a thinner layer on the flank to the Siberian side. The gray layer is also thinner to the Greenland side of the Lomonosov Ridge and on the Morris Jesup Rise. An explanation for the huge variation in thickness is probably the transport mechanism, icebergs and sea-ice. When the sediment loaded ice is melting and depositing the material, this probably does not happen in an even manner. Especially not if the ice source is a collapsed ice-dammed lake with loads of material incorporated in the ice from a small area compared to the assumed more "normal loaded ice" from the surrounding areas. The variations in vertical position of the boundary from 30 cm in core 96/19-2pc, as mentioned above; to ca 190 cm in core 96/13-1pc at the Central Lomonosov Ridge, are probably partly due to problems with recovery, e.g. liner implosion, but also due to local differences in sedimentation rate. Core PC-08, GC-09 and GC-10 from the Morris Jesup Rise hold a gray layer with a base boundary around 50 cm in all three cores, indicating a more even infusion of material to this area, an expected consequence due to the

mixing of heavy loaded ice and less loaded ice on the long journey from the outburst area to the deposition site.

5.3 The Ice Dammed lakes as a proposed source for the Gray Layer

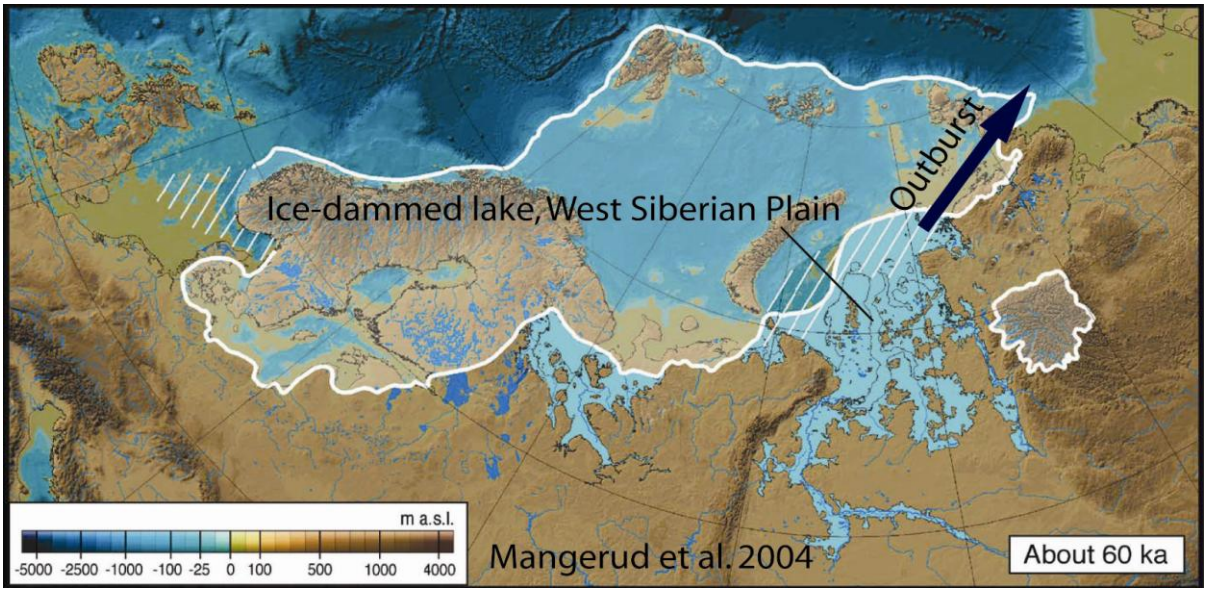

Fig. 15 Reconstruction of ice-dammed lakes during Middle Weichselian, about 60-50 ka (Mangerud et al., 2004). Ice margin (Svendsen et al., 2004) in hatched area, position of ice-margin is unknown. Dark blue arrow marks the hypothesized outburst pathway. Sea level is lowered 60 m.

At about 53 ka the ice cap had melted to a point where the water pressure exceeded the heavy load of the ice was reached, resulting in the formation of submarine drainage tunnels between the ice and the ground. Soon the whole ice margin would have collapsed due to an accelerating discharge of the lake and heavy erosion in the ice tunnels. Huge amounts of material, from clay fraction to gravel and bigger, are incorporated and mixed with glacial and sea ice. This collapsed ice mixed with sediments that were flushed out in the east side of the Nansen Basin and in to the Laptev Sea (sea level lowered by 50 m (Lambeck et al., 2002)) where the Transpolar Drift is taking over as the main ice transporter (fig. 1).
When using the modeled ice-sheet thickness and extension (Svendsen et al., 2004) for 60 ka, the only reasonably path of an outburst from the lake on the west Siberian Plain around 53 ka seems to be between the northeastern part of the ice sheet at the Kara Sea shelf and the Taimyr Peninsula (fig. 16) were the ice sheet were thin enough to lift and break. An outburst in the Barents Sea seems unlikely due to this ice sheets maximum height right in the middle of the sea. Based on clay mineral analysis, Spielhagen et al. (2004) also suggest the Western Laptev and Eastern Kara Sea as source area for this layer.

If the source area is the ice dammed lake on the West Siberian Plain and the surface currents (the Transpolar Drift) were similar to the present situation as suggested by (Bischof and Darby, 1997), the suggested position for the drainage by Mangerud (2004) to in the Kara sea is hard to accept. It postulates that the sediment loaded ice to has been flushed out in the Nansen Basin

vest of the islands Severnaya Zemlya and thereby transported in a counter current manner to be deposited on the Siberian side of the Lomonosov Ridge.

To get an idea if the volume of the gray layer and if the lake on the West Siberian Plane is reasonable as a source, seen in a physiographic-provinces-sours-area point of view, a rough calculation is done. The gray layer is set to an average thickness of 15 cm within the area, in a largest extension scenario of the whole Eurasian Basin minus shelf areas (1188×10^3 km^2; Jakobsson et al 2003) gives a gray layer volume of 178 km^3. This volume divided by the lake area, 610×10^3 km^2 (Mangerud et al., 2004), gives the erosion in the lake necessary to produce the gray layer to be less than 30 cm. Two more scenarios are presented in table 4.

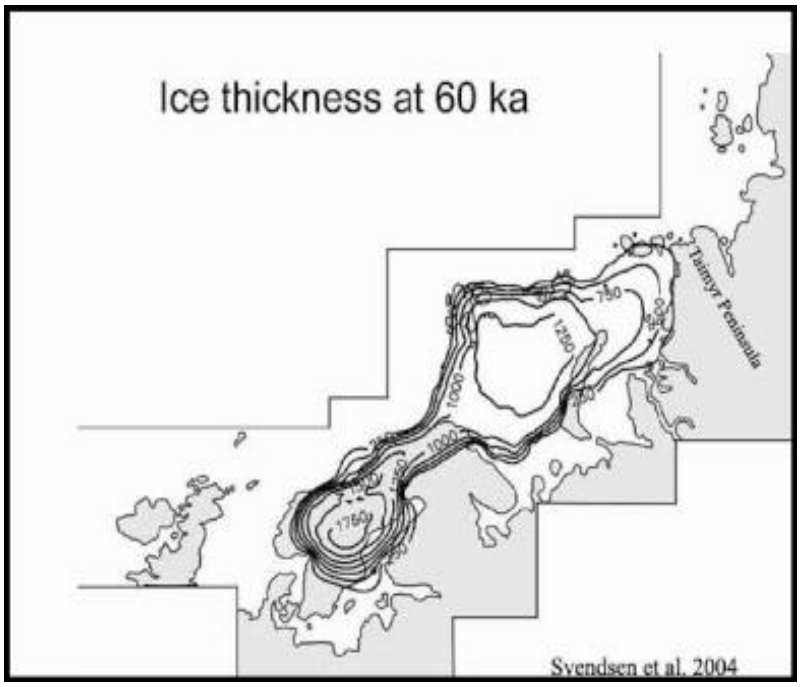

Fig. 16. Modelled ice-sheet thicknes for the early Weichselian 60 ka (Svendsen et al 2004).

Table 4. A rough calculation gives a clue about the proportion of sediment from the Lake on the West Siberian Plane needed to create the Gray Layer in the Arctic. Nine different scenarios are presented here; thickness of the layer is set to 10, 15, and 50 cm, respectively, and the extension of the layer is set to three different provinces (left column).

Gray layer extension in the Arctic	Gray layer proportion in the lake (m) when the thickness of the layer is set to 10 cm (sea)	Gray layer proportion in the lake (m) when the thickness of the layer is set to 15 cm (sea)	Gray layer proportion in the lake (m) when the thickness of the layer is set to 50 cm (sea)
Lomonosov-, Gakkel Ridge, Amundsen-, Nansen Basin.	0.19	0.29	0.97
Lomonosov-, Gakkel Ridge and Amundsen Basin	0.15	0.22	0.73
Lomonosov- and Gakkel Ridge	0.1	0.15	0.49

5.4 The chemical fingerprint

The Mn-minima used to identify the gray layer (fig. 9) is thought to be an indication of a redox-front created when the layer were deposited. The assumed quick sedimentation rate of the gray layer (Spielhagen et al., 2004), furthermore supported by the escape trace just beneath the base

boundary in core AO96-14gc (fig.14), created anoxic conditions in the pore waters that dissolved the Mn. The Mn moved in the sediment by diffusion and precipitated in the oxygenated area above and below the Gray Layer. Cr, V, Co and Ni are other redox-sensitive elements that confirm the picture of the Mn-minima to have been caused by a redox-front (fig. 17).

To obtain more definite proof for the ice-dammed lakes as source for the gray layer, clay mineral analysis of the gray layer is necessary. If the material in the Gray layer can be shown to originate primarily from a single source, this would be a strong indication that the Gray Layer is the result of an abrupt depositional event best explained by a catastrophic flooding from an ice-dammed lake. However, a much better constrained age model for the duration of this depositional event is direly needed.

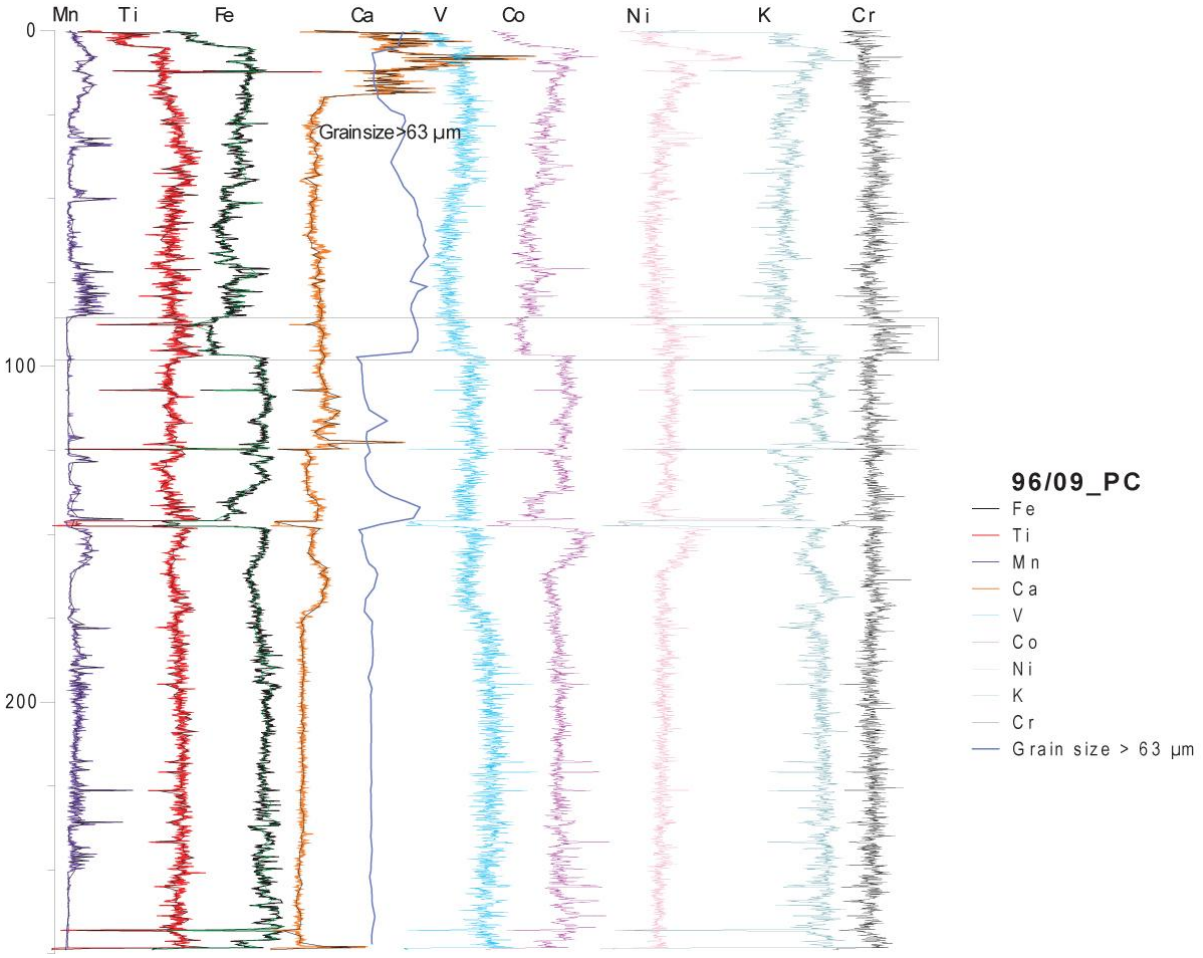

Fig. 17. Shows the chemical fingerprint used to identify the gray layer Core 96/09-1pc; Mn, Ti, Fe and Ca; grain size and five other redox sensitive elements; V, Co Ni and Cr all five shows significant change within the gray layer, marked by a rectangle, confirm the picture of the Mn-minima to have been caused by a redox front.

5.5 Future studies of the Gray Layer

Future studies of the Gray Layer and its potential connection to outbursts from ice dammed lakes on the Siberian hinterland should focus on the source region of the material in the Gray

Layer. The smectite clay mineral group was used by Vogt et al. (2001;2007) to determine the source areas for sediments in the Barents- Kara and Laptev shelf seas. This method even allowed distinct transport mechanisms and sedimentation processes to be established (Vogt 1997). The erosion products of the Putorana Trap Basalt Plateau are one of the key contents in this method (Vogt et al. 2008). The huge ice dammed lake on the west Siberian Plain was located just west of the Putorana Plateau. Thus, if the gray layer can be shown to contain large amounts of erosional products from this area, this would make the ice-dammed lake a strong candidate as the cause of the Gray Layer.

5.6 Possible climate impact du the outburst of the Ice dammed lake.

The gray layer is marker of a regime shift due to grain size and other mineral. Is the outburst of the lake the trigger of the climate anomalies or were the climate anomaly the cause of the outburst and the gray layer? The huge amount of freshwater flushed out in the arctic probably had some impact on the thermohaline circulation and formation of North Atlantic Deep Water, similar to the 100 years-long decrease in formation of NADW 8200 year ago caused by the outburst of Lake Agassiz (Kleiven and O. Richter, 2008). However, to assess the climatic impact of the "Gray Layer" outburst, a much better chronostratigraphic constraint is needed.

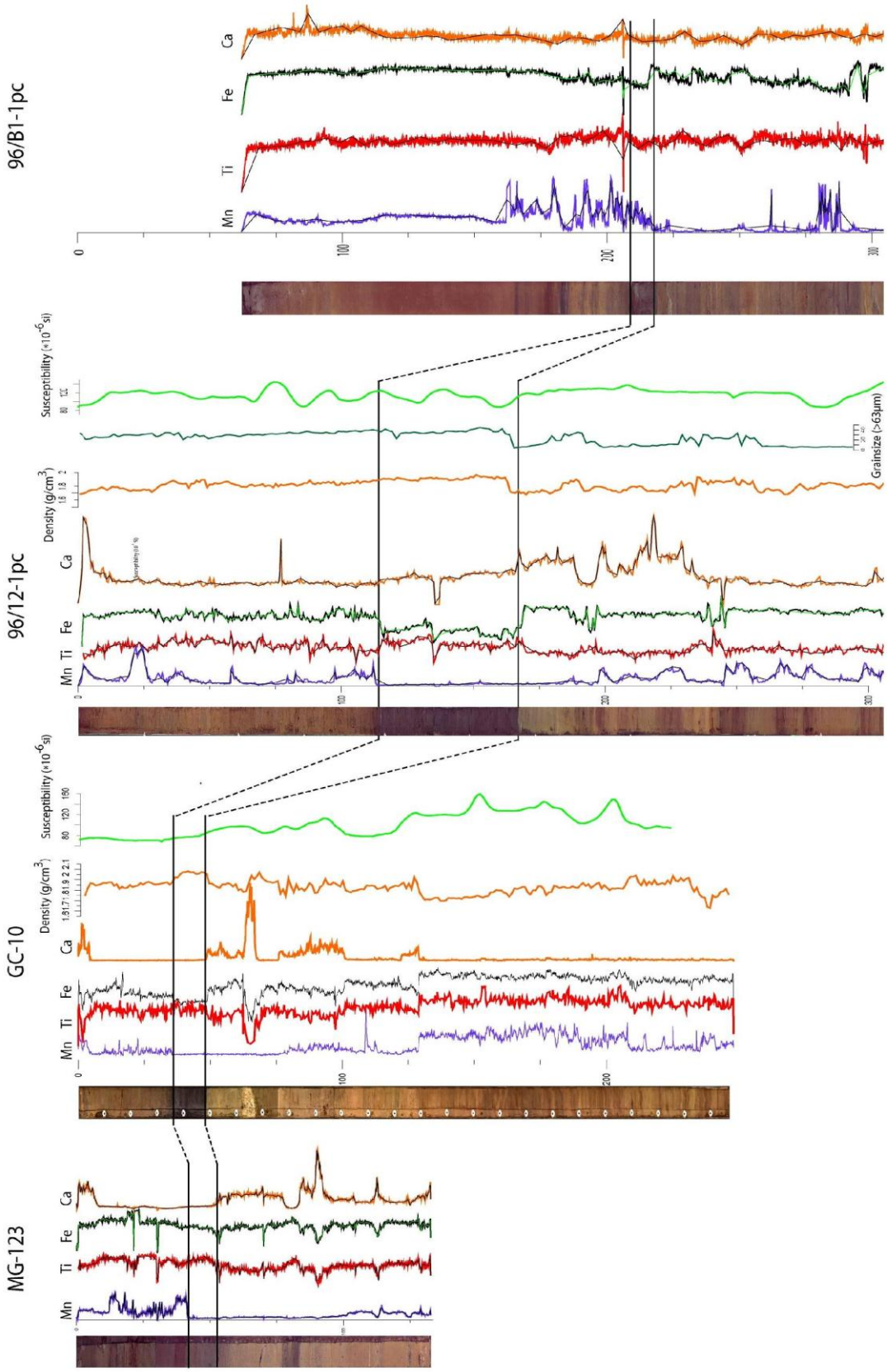

Fig. 18. Correlation between, from the left to right, the Fram Strait core MG-123, GC-10 from Morris Jesup Rise, the reference core from the Central Arctic Ocean 96/12-1pc and core 96/B1-1pc taken on the Amundsen edge of the Lomonosov Ridge west of the Oden Spur.

6. Conclusions

- The gray layer is present in the major part of the Eurasin basin, including the Lomonosov Ridge, Gakkel Ridge, Morris Jesup Rise and the Fram Strait. Contingently even present on the Mendelev Ridge in the Amerasian side of Arctic.

- The thickness of the gray layer varies considerably, from 70 cm to 2-3 cm, over rather small distances, indicating rapid and heterogeneous deposition.

- The chemical fingerprint of Mn, Fe and Ti is a distinct and significant marker of the gray layer.

- The distinct Mn minima connected to the Gray Layer is caused by anoxic conditions, resulting in a redox front that moves the Mn in the sediment.

- The onset and the sedimentation of the gray layer were rapid.

- Sours area for the gray layer is the eastern Kara- and western Laptev Sea.

- The gray layer is most probably caused by an outburst of an ice-dammed lake on the West Siberian Plain ca. 53 ka ago.

7. Acknowledgement

I wish to thank my head supervisor Ludvig Löwemark for instructions, analyses and review my second supervisor Martin Jakobsson for analyses and inspiration, Joyanto Routh for analyses. I also wish to thank Kungliga Skogs och Lantbruks Akademin for the scholarship I received that made it possibly to present these results at AGU-2008 in San Francisco.

8. References

Aagaard, K., J.H. Swift, and E.C. Carmack, 1995. Thermohaline circulation in the arctic mediterranean seas. journal of Geophysical Research, 90: 4833-4846.

Arctic Monitoring and Assessment Programme. AMAP Assessment Report: Arctic Pollution Issues, AMAP: Oslo, Norway, 1998.

Backman, J., Jakobsson, M., Løvlie, R., Polyak, L. and Febo, L.A., 2004. Is the central Arctic Ocean a sediment starved basin? Quaternary Science Reviews, 23(11 - 13): 1435 - 1454.

Bischof, J. and Darby, D., 1997. Mid- to Late Pleistocene Ice Drift in the Western Arctic Ocean: Evidence for a Different Circulation in the Past. Science, 277(5322): 74-78.

Björnsson, H., 2002. Subglacial lakes and Jökulhlaups in Iceland Global and Planetary Change, 35: 255-271.

Boström, K. and Thiede, J., 1984. YMER-80 Swedish Arctic Expedition, Cruise report for marine geology and geophysics. 260, Geologiska Institutionen, Stockholm.

Brouwer, P., 2003. Theory of XRF Getting acqainted with the priciples. PANalytical B.V.

Clark, D.L., 1970. Magnetic Reversals and Sedimentation Rates in the Arctic Ocean. Geological Society of America Bulletin, 81: 3129 - 3134.

Eiliv Larsen, S.F.a.J.T., 1999. Late Quaternary history of northern Russia and adjacent shelves — a synopsis. Boreas, 28: 6-11.

Grosswald, M.G., 1980. Late Weichselian ice sheets of northern Eurasia. Quaternary Research, 13: 1-32.

H. Sagen, S.S., P. Worcester, M. Dzieciuch and E. Skarsoulis, 2008. The Fram Strait acoustic tomography system. Acoustics'08 Paris.

Helga (Kikki) Flesche Kleiven, C.K., Carlo Laj, Ulysses S. Ninnemann, and Thomas O. Richter, E.C., 2008. Reduced North Atlantic Deep Water Coeval with the Glacial Lake Agassiz freshwater Outburst. Science, 360.

Ian W. Croudace, A.R., R. Guy Rothwell, 2006. ITRAX: description and evaluation of a new multi-function

X-ray core scanner. New Techniques in Sediment Core Analysis., Special Publications: 51-63.

Jackson, H.R., Johnson, G.L., Sundvor, E. Myhre, A.M, 1984. The Yermak Plateau: formed at a triple junction. Journal of Geophysical Research, 89: 3223-3232.

Jakobsson, M., 1999. First high-resolution chirp sonar profiles from the central Arctic Ocean reveal erosion of Lomonsov Ridge sediments. Marine Geology, 158: 111-123.

Jakobsson, M., 2002. Hypsometry and volume of the Arctic Ocean and its constituent seas. Geochemistry, Geophysics, Geosystems, 3(5): 1-18.

Jakobsson, M., 2008. Year book 2007, Swedish Polar Research Secretariat

Jakobsson, M., Grantz, A., Kristoffersen, Y. and Macnab, R., 2003. Physiographic provinces of the Arctic Ocean seafloor. GSA Bulletin, 115(12): 1443-1455.

Jakobsson, M. et al., 2000. Manganese and color cycles in Arctic Ocean sediments constrain Pleistocene chronology. Geology, 28: 23-26.

Jakobsson, M. et al., 2001. Pleistocene stratigraphy and paleoenvironmental variation from Lomonosov Ridge sediments, central Arctic Ocean. Global and Planetary change, 31(1 - 4): 1 - 22.

Kennett, J.P. and Shackleton, N.J., 1975. Laurentide ice sheet meltwater recorded in Gulf of Mexico deep-sea cores. Science, 188: 147-150.

Lambeck, K., East, T.M. and Potter, E.-K., 2002. Links between climate and sea levels for the past three million years. Nature, 419(6903): 199 - 206.

Löwemark, L., Jakobsson, M., Mörth, M. and Backman, J., 2008. Arctic Ocean Mn contents and Sediment Color Cycles. Polar Research.

Löwemark, L. and Werner, W., 2001. Dating errors in high-resolution stratigraphy:a detailed X-ray radiograph and AMS- ^{14}C study of *Zoophycos* burrows. Marine Geology, 177: 191-198.

Mangerud, J., Astakhov, V., Jakobsson, M. and Svendsen, J.I., 2001. Rapid Communication Huge Ice-age lakes in Russia. Journal of Quaternary Science, 16(8): 773 - 777.

Mangerud, J. et al., 1998. Fluctuations of the Svalbard-Barents sea ice sheet during the last 150 000 years Quaternary Science Reviews 17: 11-42.

Mangerud, J. et al., 2004. Ice-dammed lakes and rerouting of the drainage of Northern Eurasia during the last glaciation. Quaternary Science Reviews, 23: 1313-1332.

Mysak, L.A., 2001. Patterns of Arctic Circulation. Science, 293(5533): 1269 - 1270.

Peterson, B.J. et al., 2002. Increasing River Discharge to the Arctic Ocean. Science, 298(5601): 2171 - 2173.

Sohn, R.A. et al., 2008. Explosive volcanism on the ultraslow-spreading Gakkel Ridge, Arctic Ocean. Nature.

Spielhagen, R.F. et al., 2004. Arctic Ocean deep-sea record of northern Eurasian ice sheet history. Quaternary Science Reviews, 23: 1455-1483.

Spielhagen, R.F. et al., 1997. Arctic Ocean evidence for late Quaternary initiation of northern Eurasian ice sheets. Geology, 25: 783-786.

Stein, R., 1998. Arctic Paleo-River Discharge (APARD). Ber. Polarforsch 279.

Svendsen, J.I. et al., 2004. The late Quaternary ice sheet history of Nortern Eurasia, Quaternay Science Reviews special QUEEN volume. Quaternary Science Reviews, 23(11-13): 1229-1271.

Vogt, P.R., Taylor, P.T., Kovacs, L.C. and Johnson, G.L., 1979. Detailed Aeromagnetic Investigation of the Arctic Basins. Journal of geophysical research, 84(B3): 1071 - 1089.

Vogt, C., Knies, J. 2008. Sediment dynamics in the Eurasian Arctic Ocean during the last deglaciation - The clay mineral group smectite perspective. Marine Geology, 250, 3-4, pp. 211-222.

Vogt, C., 1997. Regional and temporal variations of mineral assemblages in Arctic Ocean sediments as climatic indicator during glacial/interglacial changes. Rep. Polar Res. 251, 335.